Article

pubs.acs.org/Biomac

# Mechanical Performance of Spider Silk Is Robust to Nutrient-Mediated Changes in Protein Composition

Sean J. Blamires,*[,†,‡] Chen-Pan Liao,[†] Chung-Kai Chang,[§] Yu-Chun Chuang,[§] Chung-Lin Wu,[∥] Todd A. Blackledge,[⊥] Hwo-Shuenn Sheu,[§] and I-Min Tso[†]

[†]Department of Life Science, Tunghai University, Taichung 40704, Taiwan

[‡]Evolution & Ecology Research Centre, School of Biological, Earth & Environmental Sciences, The University of New South Wales, Sydney 2052, Australia

[§]National Synchrotron Radiation Research Center, Hsinchu 3000, Taiwan

[∥]Center for Measurement Standards, Industrial Technology Research Institute, Hsinchu 30011, Taiwan

[⊥]Department of Biology, Integrated Bioscience Program, The University of Akron, Akron, Ohio 44325, United States

Supporting Information

**ABSTRACT:** Spider major ampullate (MA) silk is sought after as a biomimetic because of its high strength and extensibility. While the secondary structures of MA silk proteins (spidroins) influences silk mechanics, structural variations induced by spinning processes have additional effects. Silk properties may be induced by spiders feeding on diets that vary in certain nutrients, thus providing researchers an opportunity to assess the interplay between spidroin chemistry and spinning processes on the performance of MA silk. Here, we determined the relative influence of spidroin expression and spinning processes on MA silk mechanics when *Nephila pilipes* were fed solutions with or without protein. We found that spidroin expression differed across treatments but that its influence on mechanics was minimal. Mechanical tests of supercontracted fibers and X-ray diffraction analyses revealed that increased alignment in the amorphous region and to a lesser extent in the crystalline region led to increased fiber strength and extensibility in spiders on protein rich diets.

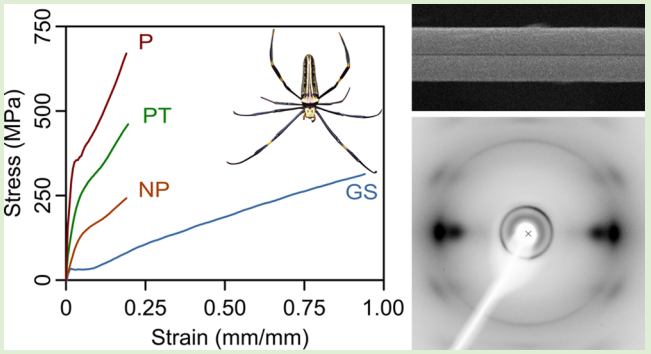


## INTRODUCTION

Spider major ampullate (MA) silk is a unique material in having both high strength and extensibility.[1−4] Its toughness, accordingly, exceeds that of any known natural or synthetic fiber. For this reason, understanding and mimicking the way spiders process MA silk to produce fibers with variable properties is considered the "holy grail" of bioengineering.[4−7] While technological advances in synchrotron X-ray diffraction and nuclear magnetic resonance (NMR) techniques have enabled insights into silk synthesis across hierarchical scales,[7−10] there is still much to be learned regarding how silks vary within and between individuals.[7,11]

MA silk comprises two proteins or spidroins. Spidroin 1, or MaSp1, contains multiple $(GA)_n$, $(GGX)_n$, and $(A)_n$ repeated amino acid sequences.[12,13] NMR and atomistic models predict that these sequences promote crystalline $\beta$-sheets in the assembled fibers.[14−16] Spidroin 2, or MaSp2, however, consists of multiple $(GPGXX)_n$ repeated sequences.[13,17] Atomistic models predict that the proline in MaSp2 inhibits $\beta$-sheet formation and promotes the formation of crystalline $\beta$-spirals and type-II $\beta$-turns in the assembled fiber.[16−19] The formation of crystalline $\beta$-sheets is promoted by MaSp1 expression, so this spidroin is thought to give the silk strength. However, the $\beta$-spirals and $\beta$-turns promoted by MaSp2 expression are thought to give the silk extensibility.[13,16] The MaSp model, accordingly, predicts that the mechanical properties of MA silk are a consequence of the ratio of MaSp1 and MaSp2 expression.

Individual MA silks vary in properties in different environments and when spiders feed on different food or take up different quantities of specific nutrients. MA silk mechanical properties may vary depending on the concentration of protein consumed by the spider,[20] offering researchers a way to understand the mechanisms by which MaSp1/MaSp2 expression can influence silk mechanics at multiple levels.[10,20−22] The variations in properties may be partly explained by protein deprivation inducing the down-regulation of MaSp2 expression.[20,21,23] Nevertheless, changes in spidroin composition need not necessarily correlate with changes in mechanics.

Physiological and biochemical processes at different sites in the silk duct during spinning affect silk properties by inducing

Received: January 4, 2015
Revised: March 9, 2015
Published: March 12, 2015






DOI: 10.1021/acs.biomac.5b00006
*Biomacromolecules* 2015, 16, 1218−1225

variations at nanoscales. For instance, the proportion and orientation of the crystals and the formation of $\beta$-sheets, $\beta$-spirals, $\beta$-turns, $3_1$-helices, and other structures are affected by variations in ion concentration and pH within the duct.[24−26] Furthermore, shear stress at the valve prior to drawing further induces molecular alignment within the crystalline and amorphous regions.[24,27,28] Amorphous region alignment may be extenuated by the spider eliciting friction on the fiber via contraction of a valve at the spigot during spinning.[20,24,29] An index of amorphous region alignment in MA silk can henceforth be measured by exposing the silk to water and measuring its capacity to supercontract, i.e., shrink and become rubbery.[9]

We, unfortunately, do not know the relative roles of MaSp expression and spinning processes on within-individual variation in MA silk mechanical properties. Here, we aim to bridge this knowledge gap by feeding the orb-web spider *Nephila pilipes* either protein rich or protein deprived solutions[20,21] before subjecting its MA silk to chromatographic analysis, native and supercontracted mechanical tests, and wide-angle X-ray diffraction analysis.

## MATERIALS AND METHODS

**Spider Collection and Pretreatment.** We collected 80 penultimate instar female *N. pilipes* (15−20 mm in body length) near Taichung City, Taiwan, between July and September 2012 and returned them to Tunghai University, Taichung. We measured their body length to ±0.1 mm using digital calipers and mass to ±0.001g using an electronic balance before placing them in 120 mm (wide) × 90 mm (high) plastic circular containers. The containers had perforated wire mesh lids with a 20 mm long slit cut into the mesh screen using a Stanley knife to facilitate feeding with a 20 $\mu$L micropipette. We fed all of the spiders 20 $\mu$L of a 30% w/v sugar solution daily over 5 days (for more details, see Blamires et al.[20,30]) to standardize their diet prior to experimentation. We weighed all spiders before and after the pretreatment to ensure individuals of approximately equal mass (one spider with a mass that deviated >50% from the mean was discarded) were used in the ensuing experiments.

**Experiment.** Following the pretreatment, we randomly divided the spiders into two groups of 40 individuals to be fed one of two solutions: a protein rich (P) or protein deprived (NP) solution, over 10 days. The protein rich solution was a mixture of 10 g of an albumin solution with 6 g of sucrose in 60 mL of water. The protein deprived solution was 8 g of sucrose in 30 mL of water. As protein and carbohydrates contain approximately similar energy densities (~4 kJ $g^{-1}$), the energy concentration across treatments was approximately similar (0.53 $kJml^{-1}$). We thus excluded the possibility that differences in energy intake influenced the silk properties across treatments.

We fed the spiders by placing a measured droplet of solution onto their chelicerae using a 20 $\mu$L micropipette (see Blamires et al.[30]). After completing the feeding experiment, we reweighed all spiders, and spiders that lost more than 20% of their mass during feeding ($n$ = 4; 2 from the P treatment and 2 from the NP treatment) were not used any further.

**Silk Extraction and Amino Acid Determination.** We anaesthetized each spider using $CO_2$ and reeled a single MA silk fiber from their spinnerets using tweezers and taped it to a mechanical spool spun at a constant speed (1m $min^{-1}$). All silks were extracted under controlled temperature (~25 °C) and humidity (~50% R.H.) in still air, so reeling speed and the postspin environment had no influence on any subsequent variations in the mechanical properties of the silks.

For ~10 individuals per treatment, we ran the spool for 1 h. We weighed the collected silk to the nearest 0.01 mg on an electronic balance before placing it into 100 $\mu$L Eppendorf tubes and submerged it in 99% hexofluoro-isopropanol solvent (500 $\mu l$ of per mg of silk) overnight. The samples were placed in glass tubes and hydrolyzed in 6 mol $L^{-1}$ HCl for 24 h in a furnace at 115 °C before the mole percentages of glutamine, serine, proline, glycine, and alanine, the amino acids representing ~90% of the total amino acids of MA silks in most spiders,[5] were determined using high performance reverse-phase liquid chromatography (HPLC, Waters Pico-Tag Amino Acid Column, Milford CA, USA).[31]

**Mechanical Tests.** We spooled the silk of ~20 spiders per treatment for 10 min. We used these samples to mount ten 25 mm lengths of taut silk fiber (thus creating 400 samples: 10 fibers each from 20 spiders from each of the two treatments) onto cardboard frames (open area = 20 × 20 $mm^2$, border = 5 mm), with double-sided adhesive tape around its border. A second cardboard frame with double-sided adhesive tape around its border was placed on top of the original, and the frames were stuck together securing the silk within by adding a drop of Elmer's glue at the position where the silk was secured between frames, and we gently squeezed the borders together with forceps. The frames containing silk were taped to a microscope slide and examined and photographed under 1000× magnification using a polarized light microscope (BX 50, Olympus, Tokyo, Japan) connected to a UC-series Nikon digital camera. We determined the width of each thread from the photographs using ImageJ (NIH, Bethesda MD, USA) to account for it in the ensuing mechanical tests.

Native silk mechanical tests were performed under controlled temperature and humidity on 10 frame-mounted silk samples from each of the 20 spiders per treatment. The tests were conducted within 14 days of their collection. We first placed the frames containing single silk fibers within the grips of a UTM Nano Bionix tensile testing machine (MTS Systems Corporation, Oakridge TN, USA), ensuring that the grips held the silk firmly at the edge of the frame. The silks were then stretched at a rate of 0.1 $mms^{-1}$ until the fiber ruptured. The load resolution was to approximately 2 $\mu$N.

True stress ($\sigma$) and strain ($\varepsilon$) were calculated using the following equations:[32]

$$\sigma = \frac{F}{A}$$

and

$$\varepsilon = \log \mathrm{e}\frac{L}{L_0}$$

where $F$ is the force applied to the specimen, and $A$ is the cross-sectional area of the thread calculated from the diameter, assuming a constant thread volume,[33] $L$ is the instantaneous length of the fiber at a given extension value, and $L_0$ is the original gauge length of the fiber.

Stress−strain curves were plotted for each silk tested using TestWorks 4.0 (MTS Systems Corporation, Eden Prairie MN, USA), from which we calculated the following mechanical properties: (1) ultimate strength or the stress at rupture; (2) extensibility or the strain at rupture; (3) toughness, the total work of extension, calculated as the area under the stress strain curve; and (4) Young's modulus (stiffness), calculated as the slope of the curve during the initial elastic phase for each specimen.

We performed supercontracted mechanical tests on a further 10 silk samples from each of the 20 spiders per treatment. The rationale for the supercontracted tests was, first, to ascertain the capacity to supercontract in water; measured as the shrink percentage[9,34] of the silks in response to variations in MaSp expression between treatments. Second, the supercontracted state represents a ground state for MA silk, where the effects of the amorphous region alignment on mechanical properties are removed.[8,34] Thus, by comparing the mechanics of supercontracted and native silk, we could ascertain the relative influence of amorphous region alignment over mechanical properties.

To ascertain the shrink percentage, we supercontracted the fibers at 100% relative humidity within a stainless steel chamber[35] while they were being held within the grips of a UTM Nano Bionix tensile tester without tension applied. We ascertained how much stress was generated when the silks were restrained, then the fibers were relaxed


DOI: 10.1021/acs.biomac.5b00006
Biomacromolecules 2015, 16, 1218−1225

while wet, and the shrink percentage was calculated as the difference between the preshrink ($l_0$) and postshrink ($l_1$) fiber lengths.[34] We then dried the fibers at maximum relaxation, upon which they were subjected to mechanical testing as outlined for native silks.

**X-ray Diffraction.** We spooled the silks of a further 10 spiders per treatment onto 3 mm × 1 mm steel frames with a 0.5 mm × 0.5 mm window for ∼2 h, ensuring that approximately 2000 rounds of silk were wrapped around each frame. We performed wide-angle X-ray diffraction analyses on the silks at the BL01C2 beamline at the National Synchrotron Radiation Research Center, Hsinchu, Taiwan. To minimize air scattering, the samples were placed inside a transparent helium-filled chamber aligned parallel to a detector at a distance of 300 mm from the incident beam. The wavelength of the incident X-ray beam was 1.033 Å. The beam size was confined by a collimator 0.5 mm in diameter. Two-dimensional diffraction patterns were recorded for each silk sample by a Mar 345 imaging plate with an exposure period of 10−60 min depending on the premeasured signal intensity. One-dimensional diffraction profiles were developed from the two-dimensional images using Fit2D software and examined for outlying data; one P treatment datum was subsequently removed prior to analyses. We calculated the (i) diffraction angles ($2\theta$), (ii) azimuthal angles, (iii) intensity peaks ($I_x$), and (iv) full width and half width maximum intensities (fwhm) $2\theta$ and azimuthal angles, to asses crystalline region alignment for the (0 2 0) and (2 1 0) Bragg reflection vectors (the vectors associated with scattering from the crystalline $\beta$-sheets[9]) from the one-dimensional diffraction profiles. We then calculated the following: (i) crystal size, $\tau$, using Scherrer's equation:[36]

$$\tau = K\lambda/\beta \cos\theta$$

where $K$ is the shape factor, which we assumed was derived from a sphere, hence a value of 0.9,[37] $\lambda$ is the incident X-ray wavelength, $\beta$ is full line widths at half the maximum intensity after subtracting the instrumental broadening, and $2\theta$ is the diffraction angles of the (0 2 0) and (2 1 0) reflection vectors.

(ii) The relative crystalline intensity ratios $I_{020}/I_{amorphous}$ and $I_{210}/I_{amorphous}$ with $I_{020}$, $I_{210}$, and $I_{amorphous}$ representing the sum of the intensity peaks at the (0 2 0) and (2 1 0) reflection vectors[9] and the amorphous region, respectively. (iii) The crystallinity index, $X_c$, according to Grubb and Jelinski.[38] (iv) Herman's orientation function, $f_c$, using the following equation:[39]

$$f_c = (3\{\cos^2 \varphi\} - 1)/2$$

where $\varphi$ is the angle between the $c$ axis and the fiber axis, $\{\cos^2\varphi\}$ is the azimuthal width of the two strongest equatorial reflections (020) and (210), determined using the equation[40]

$$\{\cos 2\varphi\} = 1 - A\{\cos 2\varphi 1\} - B\{\cos 2\varphi 2\}$$

where $A = 0.8$, and $B = 1.2$.

**Analyses.** We calculated the means ± standard errors (SEs) and used separate single-factor (at two treatment levels: P and NP) repeated measures (pre- vs post-treatment) multivariate analyses of variance (rmMANOVAs), and Fisher's least significant difference posthoc analyses to determine whether (1) the mean % glutamine, serine, proline, glycine, and alanine, and (2) the mean mechanical properties, ultimate strength, extensibility, toughness, stiffness, and shrink percentage, differed across treatments. We checked for heterogeneity and sphericity in the data using Levene's tests and Mauchly's tests, respectively, and $\log_{10}$ transformed data that failed the tests before performing the rmMANOVAs. Bonferroni-corrections to $P$-values were applied, where appropriate, to account for multiple tests.

To determine the influence of MaSp expression (which we assumed to be represented by the compositional percentage of proline and alanine[13]) on mechanical properties and shrink percentage, we pooled the post-treatment data and performed a multiple regression analyses between (i) ultimate strength, extensibility, toughness, stiffness and shrink percentage, and (ii) % proline and alanine. We tested the data for normality, linearity, homoscedasticity, and singularity using Q-Q plots and scatter-plots, $\log_{10}$, or fourth-root transforming the data where necessary. We used Welch two-sample $t$ tests with posthoc Bartlett's tests to ascertain whether the crystalline parameters differed across treatments.

## RESULTS

**Amino acid Analyses.** The mean and standard errors around the mean for % glutamine, serine, proline, glycine, and

**Table 1. Comparison of the Compositional Percentage (%) of the Amino Acids: Glutamine, Serine, Proline, Glycine, and Alanine in *Nephila pilipes* Major Ampullate Silks across Experimental Treatments[a]**

| | | treatment | | |
|---|---|---|---|---|
| amino acid | pretreatment | P | NP | Fisher's LSD |
| glutamine | 6.0 ± 1.2 | 7.1 ± 1.3 | 5.4 ± 1.0 | P > NP |
| serine | 3.7 ± 0.2 | 3.9 ± 0.1 | 4.4 ± 0.1 | P = NP |
| proline | 6.8 ± 0.9 | 7.1 ± 0.6 | 5.2 ± 0.7 | P > NP |
| glycine | 46.1 ± 3.8 | 47.3 ± 0.7 | 43.8 ± 3.9 | P > NP |
| alanine | 24.4 ± 0.8 | 24.8 ± 1.3 | 26.2 ± 0.9 | NP > P |

[a]Shows means ± SE for silks from spiders after pre-treatment feeding and upon feeding on either the protein rich (P) or protein deprived (NP) solutions and outcomes of Fisher's least significant difference (LSD) post-hoc analyses.

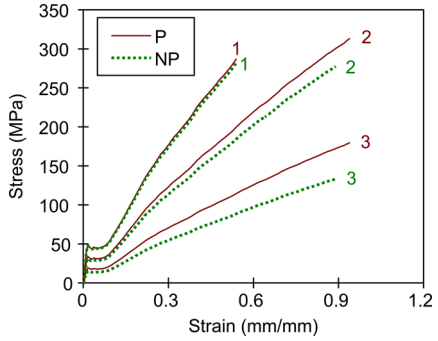


**Figure 1.** Three representative stress−strain curves of supercontracted *Nephila pilipes* major ampullate silk from protein fed (P) and protein deprived (NP) spiders (labeled 1, 2, and 3). The curves selected show the typical range of curves derived from supercontracted mechanical tests.

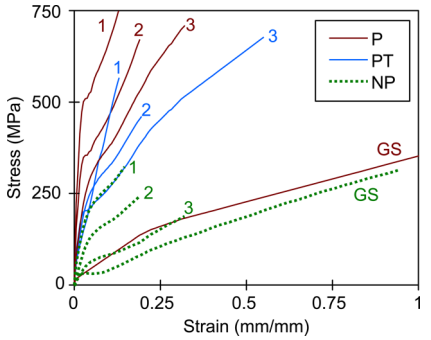


**Figure 2.** Three representative stress−strain curves of native state *Nephila pilipes* major ampullate silk from pretreatment (PT), protein fed (P), and protein deprived (NP) spiders (labeled 1, 2, and 3), and typical supercontracted (or "ground state"; labeled GS) silks of protein fed and protein deprived spiders. The curves selected show the typical range of curves derived from native state mechanical tests and average curves of the supercontracted silks.



DOI: 10.1021/acs.biomac.5b00006
*Biomacromolecules* 2015, 16, 1218−1225

**Table 2. Results of Multiple Regression Analyses between Ultimate Strength, Extensibility, Toughness, Stiffness and Shrink Percentage, and % Proline and Alanine**

| | % proline | | | % alanine | | |
|---|---|---|---|---|---|---|
| | $\beta$ | $t_{198}$ | $p$ | $\beta$ | $t_{198}$ | $p$ |
| ultimate strength (MPa) | 0.10 | 0.34 | 0.72 | 0.10 | 1.04 | 0.17 |
| extensibility (mm mm$^{-1}$) | −0.01 | −0.35 | 0.36 | 0.09 | 0.90 | 0.30 |
| toughness (MJ m$^{-3}$) | 0.18 | 0.35 | 0.72 | 0.08 | 0.10 | 0.92 |
| Young's modulus (GPa) | −0.10 | −0.44 | 0.66 | −0.10 | −1.48 | 0.12 |
| % shrink | 0.31 | 2.88 | 0.01*[a] | 0.19 | 1.80 | 0.11 |

[a]* represents significance at $p < 0.05$.

alanine that we calculated (Table 1) are comparable with previous calculations for *N. pilipes* silks using HPLC, with the possible exception that % proline (for which values of ∼8−9% have been recorded) was marginally lower.[41−44] Our analyses found that the post-treatment MA silks of spiders fed the protein rich solutions (P treatment) had greater % glutamine, glycine, and proline (rmMANOVA: Wilk's $\lambda$ = 0.408; $df$ = 16,64; $p$ = 0.001; Fisher's least significant difference tests, all $p$ < 0.05; see Table 1). The post-treatment MA silks of spiders deprived of protein (NP treatment), however, had greater % alanine. These results suggest that the MaSp1/MaSp2 ratio in the MA silk of the spiders on the two treatments differed, with significant post-treatment down-regulation of MaSp2 in the silks of spiders deprived of protein.

**Mechanical Properties.** Our native silk mechanical analysis found that the post-treatment MA silks of spiders fed the protein rich solutions had greater ultimate strength, extensibility, and Young's modulus than those of spiders deprived of protein (rmMANOVA: Wilk's $\lambda$ = 0.889; $df$ = 4,336; $p < 0.001$; Fisher's least significant difference tests, all $p$ < 0.05) (Supporting Information, Table S1).

**Supercontraction.** We found no significant differences across treatments in the mechanical properties of supercontracted silks (rmMANOVA: Wilk's $\lambda$ = 0.196; $df$ = 4,336; $p$ = 0.120) (Supporting Information, Table S2), with similar variability evident in the stress−strain curves of supercontracted silks from spiders fed the protein rich and protein deprived solutions (Figure 1). We interpreted this as being a consequence of the silks conforming to a ground state, where the effects of amorphous region alignment were removed, and the variations in amino acid compositions between treatments were never large enough to induce major differences in the mechanical properties. The shrink percentage of the silks of spiders fed each treatment significantly differed ($F$ = 3.430; $df$ = 4,336; $p < 0.001$) (Supporting Information, Table S1). Thus, the influence of amorphous region alignment on the mechanics of the native silks differed between treatments. Figure 2 shows

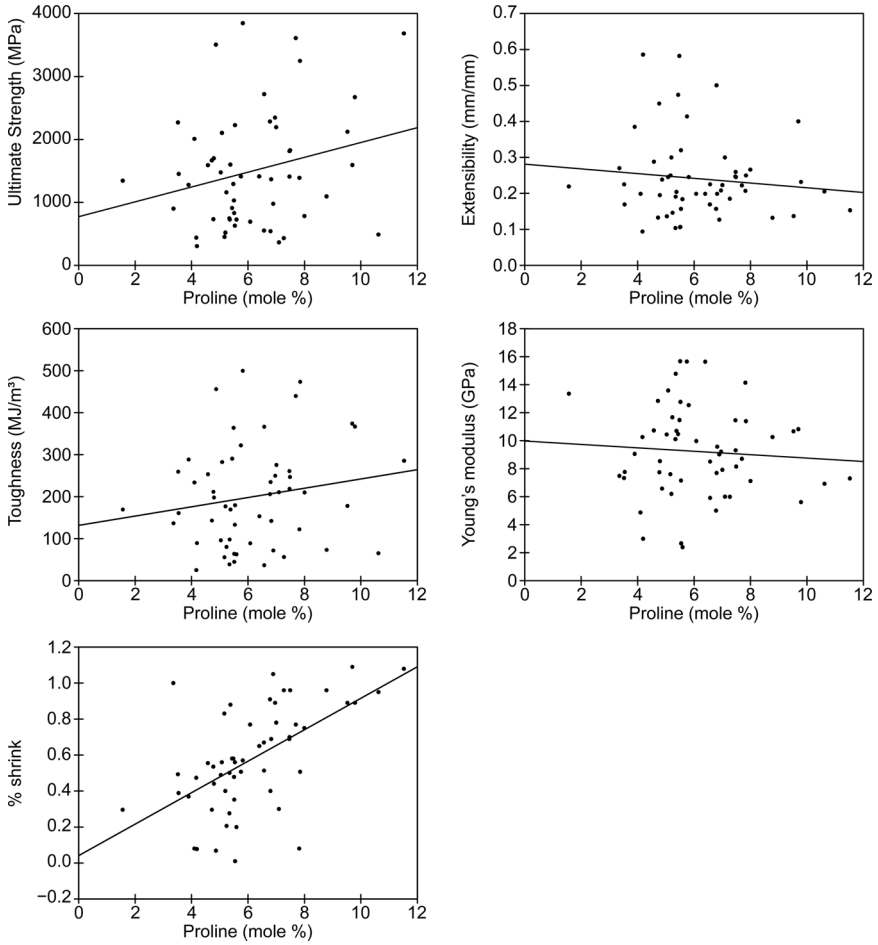


**Figure 3.** Scatterplots of silk mechanical properties ultimate strength, extensibility, Young's modulus, and % shrink vs % proline when all of the data across treatments were pooled.


DOI: 10.1021/acs.biomac.5b00006
*Biomacromolecules* 2015, 16, 1218−1225

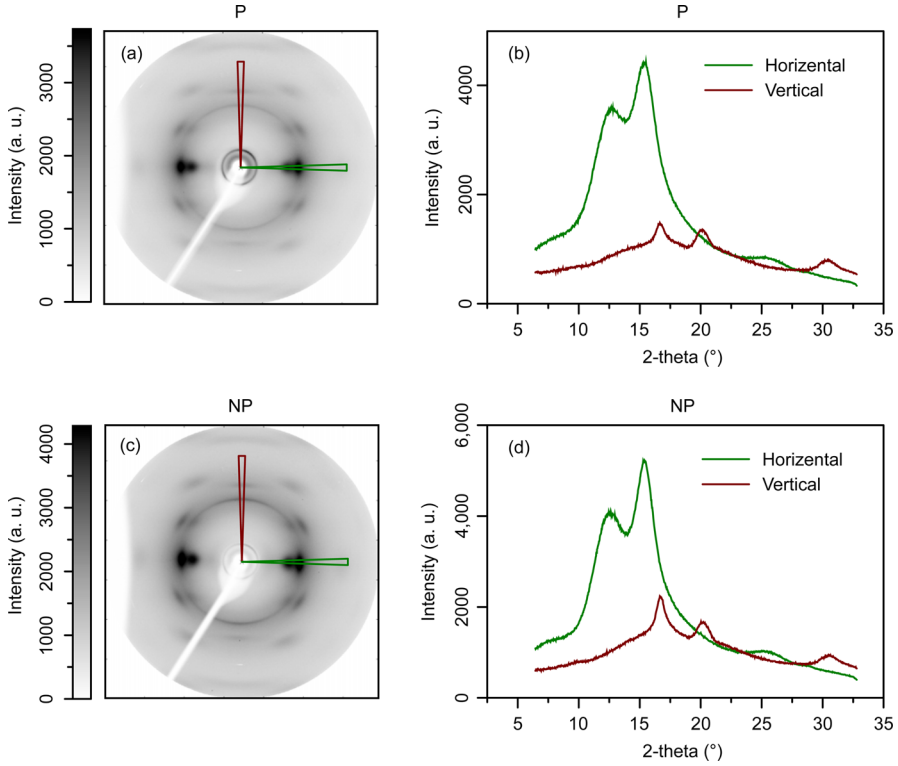


**Figure 4.** Representative X-ray diffraction profiles of *Nephila pilipes* major ampullate silks measured perpendicular to the silk axis across experimental treatments. (a) A representative two-dimensional X-ray diffraction pattern for silk from spiders fed the protein rich (P) solution. (b) An example of a diffraction intensity vs diffraction angle ($2\theta$) curve from spiders fed the protein rich (P) solution. (c) A representative two-dimensional X-ray diffraction pattern for silk from spiders deprived of protein (NP). (d) An example of a diffraction intensity vs diffraction angle curve from spiders deprived of protein (NP). Green lines in b and d represent measurements made horizontally through the (020) and (210) reflection vectors, while red lines represent measurements made vertically through the (002) reflection vector.

that the silks from each treatment were more extensible with a lower ultimate strength when in the ground state than when in the native state. Furthermore, the ultimate strength of native silks of spiders deprived of protein was similar to that of the ground state silks but was considerably lower than that for the silks from spiders fed the protein rich solutions (Figure 2).

**Influence of MaSp Expression on Mechanical Properties.** We found that shrink percentage was associated with % proline in all of the silks. We did not find any of the other silk properties, including extensilbility, to be associated with % proline or % alanine (Table 2; Figure 3). This suggests that while spidroin expression varied between the treatments it did not influence any mechanical properties aside from the silk's capacity to shrink.

**Crystalline Properties.** Representative X-ray diffraction profiles and diffraction intensity vs diffraction angle ($2\theta$) curves for silks of spiders from the P and NP treatments are shown in Figure 4. The intensity vs $2\theta$ curves revealed narrower and sharper intensity peaks at a $2\theta$ between 15° and 18° in the silks from the NP treatment. Moreover, the silks from spiders deprived of protein had significantly larger fhwm azimuthal angles at the (020) and (210) Bragg reflection vectors (Bartlett's tests: $p < 0.05$) (Figure 5a). The fwhm $2\theta$ diffraction angles, however, were insignificant at the (020) and (210) vectors. While the amorphous halo was sufficient to compare the fwhm $2\theta$ diffraction angles from the amorphous region, we could not detect a significant difference between treatments (Bartlett's tests: all $p > 0.05$) (Figure 5b). The silks from spiders fed the protein rich solutions had slightly greater relative crystal intensities ($I_{020}/I_{210}$) at the (020) and (210) reflection vectors (Figure 5c). We interpreted these results as indicative that there were differences in crystalline region alignment between silks across treatments, with spiders fed the protein rich treatment producing silks that were slightly more aligned in the crystalline region than those deprived of protein. We nevertheless found crystal size, crystallinity number, crystallinity ratio, crystallinity index, and Herman's orientation not to differ across treatments (Bartlett's tests: $p > 0.05$).

## DISCUSSION

Here, we fed the spider *Nephila pilipes* protein rich or protein deprived solutions and found a reduction in the post-treatment % glutamine, glycine, and proline in the silks of the protein deprived spiders. This finding suggests that MaSp2 expression was down-regulated when the spiders were protein deprived, confirming previous suggestions that MaSp1 is preferentially expressed when spiders are under nutritional stress.[20,23,45]

The spiders fed the protein rich solution also produced silks with a higher % proline, so there is a high abundance of the $(GPGXX)_n$ sequences, which are found exclusively in MaSp2, in their silks. An abundance of the $(GPGXX)_n$ sequences explains the greater shrinkage when supercontracted by the silks of the protein fed spiders because water molecules disrupt the hydrogen bonds between the $\beta$-spiral and $\beta$-turn conformations, thus disrupting the amorphous region alignment.[17,34,46,47] The higher shrink percentage evident in the native silks from the spiders fed the protein rich solution thus would agree with expectations of the MaSp model that MaSp1/MaSp2 expression affects mechanics. The $(GPGXX)_n$ sequence promotes $\beta$-spiral and $\beta$-turn conformations,[17] so should also


DOI: 10.1021/acs.biomac.5b00006
*Biomacromolecules* 2015, 16, 1218−1225

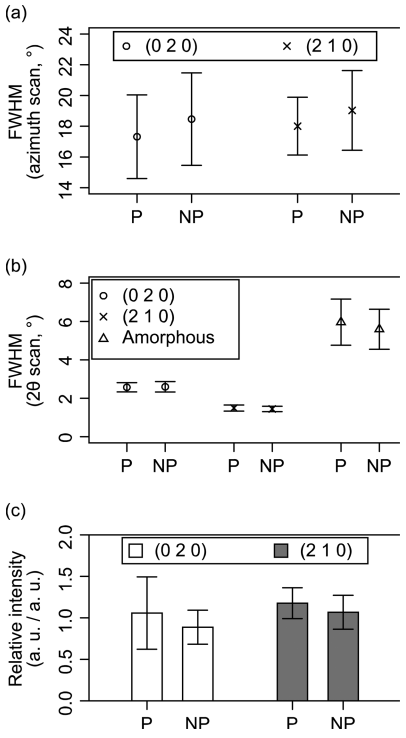


**Figure 5.** Between treatment comparison of the crystalline properties determined using X-ray diffraction. (a) Half-maximum intensity (fwhm) azimuthal angle for the (0 2 0) and (2 1 0) reflection vectors. (b) Half-maximum intensity (fwhm) of the diffraction angle ($2\theta$) for the (0 2 0), (2 1 0), and amorphous halo reflection vectors. (c) Relative crystalline intensity ratio for the (0 2 0) and (2 1 0) reflection vectors. Mean values ± SE for silks from spiders fed either a protein rich (P) or protein deprived (NP) solution are shown.

facilitate greater thread extensibility.[16,17,48] Previous studies have found a relationship between the % proline and extensibility in spider MA silk.[46,48] Our regression analyses, nevertheless, failed to find a relationship between % proline and extensibility. We thus concluded that MaSp expression had a minimal influence on silk mechanical performance.

MaSp expression alone could not explain many of the mechanical property variations that we found between treatments. For instance, the silks of spiders fed the protein rich solution were stronger and stiffer and more extensible than those of spiders deprived of protein. As these silks had more proline but less alanine, they should have had weaker and more extensible silk owing to the greater abundance of $(GPGXX)_n$ sequences.[13,16,17] We expect that the gland's physiological or biochemical mechanisms, such as variations in duct ion concentrations or pH during spinning,[24−26] induced variations in protein secondary structure, thus changing amorphous and crystalline region alignment independent of MaSp expression. Our X-ray diffraction experiments were conducted to confirm this prediction.

The proportion and orientation of the $\beta$-sheet crystalline structures and the formation of $\beta$-spirals, $\beta$-turns, $3_1$-helices, and other structures in the amorphous region are affected by physiological and biochemical processes acting in the silk duct.[25,26,49,50] We examined the alignment, intensity, size, and orientation of the crystalline $\beta$-sheets across treatments using wide-angle X-ray diffraction and found some differences. For instance, silks from the NP treatment spiders had sharper intensity peaks at a $2\theta$ between 15 and 18°, and significantly larger fhwm azimuthal angles and smaller relative crystal intensities at the (020) and (210) reflection vectors. We interpreted these as spiders fed the protein rich solution producing silks that were slightly more aligned in the crystalline region than those deprived of protein.

Our supercontraction analyses nevertheless suggested that amorphous region alignment had the greatest influence on the mechanics of the silks across treatments,[8,33,51] contrasting with our X-ray diffraction analyses, which suggested that amorphous region alignment did not vary substantially across treatments. The latter finding, however, may have been a consequence of the detection of too weak of an amorphous halo. Further analyses are thus needed using small-angle X-ray diffraction and other amorphous probing techniques to ascertain precisely how much variation there was in amorphous region alignment.

Previous studies investigating the mechanical property variations in MA silk under the influence of diet have implicated the amorphous region to be of primarily importance.[52] Our finding of significant differences in the mechanical properties of the native and supercontracted silks across treatments coupled with our findings of only slight variations in crystalline region alignment across treatments suggests that changes in the amorphous region were predominantly important in inducing property variations in *N. pilipes* silks when they consumed different quantities of protein.

## ■ CONCLUSIONS

This study systematically examined how protein intake mediates silk property changes at multiple levels. We found that spiders deprived of protein down-regulated their MaSp2 expression. The differences in MaSp expression between treatments explained the variations in shrink percentage but not strength, extensibility, or stiffness. Our X-ray diffraction analyses detected slight differences in crystalline region alignment, but we expected variations in the amorphous region alignment to be most explicable at explaining the mechanical property variations across treatments.

Despite intense interest in understanding and harnessing the properties of spider silks, attempts to create analogues have to date been unsuccessful. This failure may be attributed to a lack of control over the variation in silks spun from the protein feedstocks. Our study showed that MaSp expression shifts with protein intake but that most of the variations in mechanical properties are influenced by glandular processes affecting amorphous and, to a lesser extent, crystalline region alignment. Further wide- and small-angle X-ray diffraction examinations of single silk fibers from protein fed and protein deprived spiders will provide more information on the nature and cause of the variations.

## ■ ASSOCIATED CONTENT

### Supporting Information

Comparison across experimental treatments of the mechanical parameters, ultimate strength, extensibility, toughness, Young's modulus, and % shrink of *Nephila pilipes* major ampullate silks in the native state and when supercontracted. This material is available free of charge via the Internet at http://pubs.acs.org.

## ■ AUTHOR INFORMATION

### Corresponding Author

*E-mail: s.blamires@unsw.edu.au.



DOI: 10.1021/acs.biomac.5b00006
*Biomacromolecules* 2015, 16, 1218−1225

### Author Contributions

S.J.B and I.M.T. conceived and designed the experiments. S.J.B., C.P.L., C.K.C., and Y.C.C. performed the experiments and analyzed the data. C.L.W. and T.A.B. contributed to mechanical testing and analyses. H.S.S. contributed to X-ray diffraction analyses. All authors were involved in the preparation of this manuscript.

### Notes

The authors declare no competing financial interest.

## ■ ACKNOWLEDGMENTS

Our research was supported by National Science Council, Taiwan, grants (NSC-102-2311-B-029-001-MY3 and NSC-102-2811-B-029-001 to I.M.T and S.J.B) and an Australian Research Council (Discovery Early Career Researcher Award DE140101281 to S.J.B). We thank John Daniels and Christian Riekel for assistance with interpretation of the X-ray diffraction analyses.

## ■ REFERENCES

(1) Agnarsson, I.; Kuntner, M.; Blackledge, T. A. Bioprospecting finds the toughest biological material: extraordinary silk from a giant riverine orb spider. *PLoS One* **2010**, *5*, e11234.
(2) Bratzel, G.; Buehler, M. J. Molecular mechanics of silk nanostructures under varied mechanical loading. *Biopolymers* **2011**, *97*, 408−417.
(3) Tarakanova, A.; Buehler, M. J. A materiomics approach to spider silk: protein molecules to webs. *JOM* **2012**, *64*, 214−225.
(4) Garb, J. E. In *Spider Research in the 21st Century: Trends and Perspectives*; Penny, D., Ed.; SIRI Scientific: Manchester, U.K., 2013; pp 252−281.
(5) Lewis, R. V. Spider silk: ancient ideas for new biomaterials. *Chem. Rev.* **2006**, *106*, 3762−3774.
(6) Hardy, J. G.; Romer, L. M.; Scheiber, T. R. Polymeric materials based on silk proteins. *Polymer* **2008**, *49*, 4309−4327.
(7) Vollrath, F.; Porter, D.; Holland, C. The science of silks. *MRS Bull.* **2013**, *38*, 73−80.
(8) Elices, M.; Plaza, G. R.; Perez-Reiguero, J.; Guinea, G. V. The hidden link between supercontraction and mechanical behavior of spider silks. *J. Mech. Behav. Biomed. Mater.* **2011**, *4*, 658−669.
(9) Plaza, G. R.; Perez-Reiguero, J.; Riekel, C.; Perea, G. B.; Agullo-Rueda, F.; Burghammer, M.; Guinea, G. V.; Elices, M. Relationship between microstructure and mechanical properties in spider silk fibers: identification of two regimes in the microstructural changes. *Soft Mater.* **2012**, *8*, 6015−6026.
(10) Blamires, S. J.; Wu, C. C.; Wu, C. L.; Sheu, H. S.; Tso, I. M. Uncovering spider silk nanocrystalline variations that facilitate wind-induced mechanical property changes. *Biomacromolecules* **2013**, *14*, 3484−3490.
(11) Vollrath, F.; Porter, D.; Holland, C. There are many more lessons still to be learned from spider silks. *Soft Mater.* **2011**, *7*, 9595−9600.
(12) Xu, M.; Lewis, R. V. Structure of a protein superfiber: spider dragline silk. *Proc. Natl. Acad. Sci. U.S.A.* **1990**, *87*, 7120−7124.
(13) Sponner, A.; Schlott, B.; Vollrath, F.; Unger, E.; Grosse, F.; Weisshart, K. Characterization of the protein components of *Nephila clavipes* dragline silk. *Biochemistry* **2005**, *44*, 4727−4736.
(14) Simmons, A.; Ray, E.; Jelinski, L. W. Solid-state $^{13}C$ NMR of *Nephila clavipes* dragline silk establishes structure and identity of crystalline regions. *Macromolecules* **1994**, *27*, 5235−5237.
(15) van Beek, J. D.; Beaulieu, L.; Schafer, H.; Demura, M.; Asakura, T.; Meier, B. H. Solid-state NMR determination of the secondary structure of *Samia cynthia* ricini silk. *Nature* **2000**, *405*, 1077−1079.
(16) Creager, M. S.; Jenkins, J. E.; Thagard-Yeaman, L. A.; Brooks, A. E.; Jones, J. A.; Lewis, R. V.; Holland, G. P.; Yarger, J. L. Solid-state NMR comparison of various spiders' dragline silk fiber. *Biomacromolecules* **2010**, *11*, 2039−2043.
(17) Shi, X.; Yarger, J. L.; Holland, G. P. Elucidating proline dynamics in spider dragline silk fibre using 2H−13C HETCOR MAS NMR. *Chem. Commun.* **2014**, *50*, 4856−4859.
(18) Izdebski, T.; Akhenblit, P.; Jenkins, J. E.; Yarger, J. L.; Holland, G. P. Structure and dynamics of aromatic residues in spider silk: 2D carbon correlation NMR of dragline fibers. *Biomacromolecules* **2010**, *11*, 168−174.
(19) Jenkins, J. E.; Creager, M. S.; Butler, E. B.; Lewis, R. V.; Yarger, J. L.; Holland, G. P. Solid-state NMR evidence for elastin-like $\beta$-turn structure in spider dragline silk. *Chem. Commun.* **2010**, *46*, 6714−6716.
(20) Blamires, S. J.; Wu, C. L.; Tso, I. M. Variation in protein intake induces variation in spider silk expression. *PLoS One* **2012**, *7*, e31626.
(21) Blamires, S. J.; Tso, I. M. Nutrient-mediated architectural plasticity of a predatory trap. *PLoS One* **2013**, *8*, e54558.
(22) Boutry, C.; Blamires, S. J. In *Spiders: Morphology, Behavior and Geographic Distribution*; Santerre, M., Ed.; Nova: New York, 2013; pp 1−46.
(23) Guehrs, K. H.; Schlott, B.; Grosse, F.; Weisshart, K. Environmental conditions impinge on dragline silk protein composition. *Insect Mol. Biol.* **2008**, *17*, 553−564.
(24) Vollrath, F.; Knight, D. P. Liquid crystalline spinning of spider silk. *Nature* **2001**, *410*, 541−548.
(25) Keten, S.; Xhu, Z.; Ihle, M.; Buehler, M. J. Nanoconfinement controls stiffness, strength and mechanical toughness of $\beta$-sheet crystals in silk. *Nat. Mater.* **2010**, *9*, 359−367.
(26) Lefevre, T.; Paquet-Mercier, F.; Rioux-Dube, J. F.; Pezolet, M. Structure of silk by Raman spectromicroscopy: from the spinning glands to the fibers. *Biopolymers* **2011**, *97*, 322−335.
(27) Lele, A. K.; Joshi, Y. M.; Mashelkar, R. A. Deformation induced hydrophobicity: implications in spider silk formation. *Chem. Eng. Sci.* **2001**, *56*, 5793−5800.
(28) Hagn, F.; Eisoldt, L.; Hardy, J. G.; Vendrely, C.; Coles, M.; Scheibel, T.; Kessler, H. A conserved spider silk domain acts as a molecular switch that controls fibre assembly. *Nature* **2010**, *465*, 239−242.
(29) Vehoff, T.; Glisovic, A.; Schollmeyer, H.; Zippelius, A.; Salditt, T. Mechanical properties of spider dragline silk: humidity, hysteresis, and relaxation. *Biophys. J.* **2007**, *93*, 4425−4432.
(30) Blamires, S. J.; Sahni, V.; Dhinojwala, A.; Blackledge, T. A.; Tso, I. M. Nutrient deprivation induces property variations in spider gluey silk. *PLoS One* **2014**, *9*, e88487.
(31) Hess, S.; van Beek, J.; Pannell, L. K. Acid hydrolysis of silk fibroins and determination of the enrichment of isotopically labeled amino acids using precolumn derivatization and high-performance liquid chromatography− electrospray ionization−mass spectrometry. *Anal. Biochem.* **2002**, *311*, 19−26.
(32) Blackledge, T. A.; Hayashi, C. Y. Unraveling the mechanical properties of composite silk threads spun by cribellate orb-weaving spiders. *J. Exp. Biol.* **2006**, *209*, 3131−3140.
(33) Guinea, G. V.; Perez-Reiguero, J.; Plaza, G. R.; Elices, M. Volume constancy during stretching of spider silk. *Biomacromolecules* **2006**, *7*, 2173−2177.
(34) Boutry, C.; Blackledge, T. A. Evolution of supercontraction in spider silk: structure−function relationship from tarantulas to orb-weavers. *J. Exp. Biol.* **2010**, *213*, 3505−3514.
(35) Agnarsson, I.; Boutry, C.; Wong, S. C.; Baji, A.; Dhinojwala, A.; Sensenig, A.; Blackledge, T. A. Supercontraction forces in spider dragline silk depend on hydration rate. *Zoology* **2009**, *112*, 325−331.
(36) Riekel, C.; Branden, C. I.; Craig, C. L.; Ferrero, C.; Heidelbach, F.; Muller, M. Aspects of X-ray diffraction on single spider fibers. *Int. J. Biol. Macromol.* **1999**, *24*, 179−186.
(37) Glisovic, A.; Vehoff, T.; Davies, R. J.; Salditt, T. Strain dependent structural changes of spider dragline silk. *Macromolecules* **2008**, *41*, 390−398.
(38) Grubb, D. T.; Jelinski, L. W. Fiber morphology of spider silk: the effects of tensile deformation. *Macromolecules* **1997**, *30*, 2860−2867.


DOI: 10.1021/acs.biomac.5b00006
*Biomacromolecules* 2015, 16, 1218−1225

(39) Jenkins, J. E.; Sampath, S.; Butler, E.; Kim, J.; Henning, R. W.; Holland, G. P.; Yarger, J. L. Characterizing the secondary protein structure of black widow dragline silk using solid-state NMR and X-ray diffraction. *Biomacromolecules* **2013**, *14*, 3472−3483.
(40) Stein, R. S. *Structure and Properties of Oriented Polymers*; Wiley: New York, 1975.
(41) Tso, I. M.; Wu, H. C.; Hwang, H. C. Giant wood spider *Nephila pilipes* alters silk protein in response to prey variation. *J. Exp. Biol.* **2005**, *208*, 1053−1061.
(42) Tso, I. M.; Chiang, S. Y.; Blackledge, T. A. Does the giant wood spider *Nephila pilipes* respond to prey variation by altering web or silk properties? *Ethology* **2007**, *113*, 324−333.
(43) Blamires, S. J.; Chao, I. C.; Tso, I. M. Prey type, vibrations and handling interactively influence spider silk expression. *J. Exp. Biol.* **2010**, *213*, 3906−3910.
(44) Blamires, S. J.; Wu, C. L.; Blackledge, T. A.; Tso, I. M. Post-secretion processing influences spider silk performance. *J. R. Soc. Interface* **2012**, *9*, 2479−2487.
(45) Craig, C. L.; Hsu, M.; Kaplan, D. L.; Pierce, M. E. A comparison of the composition of silk proteins produced by spiders and insects. *Int. J. Biol. Macromol.* **1999**, *24*, 109−118.
(46) Liu, Y.; Sponner, A.; Porter, D.; Vollrath, F. Proline and processing of spider silks. *Biomacromolecules* **2008**, *9*, 116−121.
(47) Guan, J.; Vollrath, F.; Porter, D. Two mechanisms for supercontraction in *Nephila* spider dragline silk. *Biomacromolecules* **2011**, *12*, 4030−4035.
(48) Marhabaie, M.; Leeper, T. C.; Blackledge, T. A. Protein composition correlates with the mechanical properties of spider (*Argiope trifasciata*) dragline silk. *Biomacromolecules* **2014**, *15*, 20−29.
(49) Chen, X.; Shao, Z. Z.; Vollrath, F. The spinning processes for spider silk. *Soft Mater.* **2006**, *2*, 448−451.
(50) Nova, A.; Keten, S.; Pugno, N. M.; Redaelli, A.; Buehler, M. J. Molecular and nanostructural mechanisms of deformation, strength and toughness of spider silk fibrils. *Nano Lett.* **2010**, *10*, 2626−2634.
(51) Elices, M.; Guinea, G. V.; Plaza, G. R.; Karatzas, C.; Riekel, C.; Agullo-Rueda, F.; Daza, R.; Perez-Reiguero, J. Bioinspired fibers follow the track of natural spider silk. *Macromolecules* **2011**, *44*, 1166−1176.
(52) Craig, C. L.; Riekel, C.; Herberstein, M. E.; Weber, R. S.; Kaplan, D.; Pierce, N. E. Evidence for diet effects on the composition of silk proteins produced by spiders. *Mol. Biol. Evol.* **2000**, *17*, 1904−1913.


DOI: 10.1021/acs.biomac.5b00006
*Biomacromolecules* 2015, 16, 1218−1225